

Linearizing Water Molecule Using A Linearly Polarized High Intensity High Frequency Laser

Vishal Tiwari

*A dissertation submitted for the partial fulfillment of
BS-MS dual degree in Science*



INDIAN INSTITUTE OF SCIENCE EDUCATION AND
RESEARCH, MOHALI

April 2019

Certificate of Examination

This is to certify that the dissertation titled “**Linearizing Water Molecule Using A Linearly Polarized High Intensity High Frequency Laser**” submitted by **Mr. Vishal Tiwari (Reg. No. MS14017)** for the partial fulfilment of BS-MS dual degree programme of the Institute, has been examined by the thesis committee duly appointed by the Institute. The committee finds the work done by the candidate satisfactory and recommends that the report be accepted.

Professor K. S. Vishwanathan

Dr. Kamal P. Singh

Dr. P. Balanarayan
(Supervisor)

Declaration

The work presented in this dissertation has been carried out by me with Dr. P. Balanarayan at Indian Institute of Science Education and Research, Mohali. This work has not been submitted in part or in full for a degree, a diploma, or a fellowship to any other university or institute. Wherever contributions of others are involved, every effort is made to indicate this clearly, with due acknowledgement of collaborative research and discussions. This thesis is a bonafide record of original work done by me and all sources listed within have been detailed in the bibliography.

Vishal Tiwari
(Candidate)

Dated: April 2019

In my capacity as the supervisor of the candidate's project work, I certify that the above statements by the candidate are true to the best of my knowledge.

Dr. P. Balanarayan
(Supervisor)

Acknowledgements

I would like to express my gratitude to my advisor, Dr. P. Balanarayan, for his guidance and encouragement throughout my project. I also thank my project committee members, Professor K.S. Vishwanathan and Dr. Kamal P. Singh for providing many valuable comments that improved contents of this dissertation. Special thanks to Naveen for his guidance, teaching and training on the required tools to work in the lab. I thank Prashant for providing the required codes for computation. I thank my labmates Alkit, Mythreyi, Mishu, Nitin, Prateek, Rishabh, and Taseng and all the lab parties which kept me motivated to work the next day. I thank my parents, Sunil and Poonam, for constant love, guidance and strength throughout my career. I thank my friends Ajay, Kapil, Kaushal, Pranshu, Rowny, Reena and Sippy for being supportive, with whom I spent wonderful time during my degree and shared many good and bad moments of my life.

*“ OBSERVATIONS NOT ONLY DISTURB WHAT IS TO BE MEASURED,
THEY PRODUCE IT ”*

Pascual Jordan

*“ NOTHING MAKES A PERSON MORE PRODUCTIVE THAN THE LAST
MINUTE ”*

Anonymous

Dedicated to My Parents, Teachers and Friends
For love, support and encouragement

Contents

Acknowledgements	iii
List of Figures	vii
Abbreviations	x
Physical Constants	xi
Symbols	xii
1 Introduction	1
1.1 Atoms and molecules in a strong laser	1
1.2 Kramers-Henneberger atom	4
1.3 Water molecule- Geometry and electronic structure	7
1.4 Objectives and Overview	8
2 Why water should linearize in a linearly polarized light?	15
2.1 Split states	15
2.2 Electronic structure in presence of field	20
2.3 Conclusion	24
3 Linearizing water molecule	27
3.1 (t,t') method for time dependent Schrödinger equation	28
3.2 Electronic dynamics	30
3.3 Conclusion	33
A Numerical Method to solve Time dependent Schrödinger equation	35
A.1 Split operator method	35

List of Figures

1.1	(a) Equilibrium geometry for water molecule with angles and distances marked in figure, computed with geometry optimization using Moller-Plesset(second) order(MP2) method with coemd-ref basis set. MP2 energy is -76.06689 Hartree (b) Optimized linear geometry for water molecule with angles and distances marked in figure, computed using Moller-Plesset(second) order(MP2) method and coemd-ref basis set, MP2 energy is -76.01557 Hartree.	8
1.2	Barrier for water inversion for H-O-H angle variation from bent to linear geometry computed using MP2 method and coemd-ref basis. The energy difference between the bent and linear geometry using MP2 method is 1.394 eV with equilibrium geometry being bent and transition state being linear.	9
1.3	Excited states of intermediate geometries from bent to linear calculated using MP2 method and coemd-ref basis with varying coordinates from bent to linear geometry along with the ground state energy(brown plot). The excitation energy for bent geometry has been marked in the plot.	10
1.4	Absorption spectrum for water molecule in 400 – 700 nm range with a minimum in absorption at 418 nm. At this frequency, the transition dipoles are minimum and thus intensity can be cranked up at this frequency without destruction of molecule. Image taken from https://upload.wikimedia.org/wikipedia/commons/b/b5/Water_absorption_coefficient_large.gif	11
2.1	Coulomb potential(black curve) for linear geometry water molecule in presence of oscillating field with varying laser parameter α_o . Coulomb potential gets split into two as α_o is increased. Value of α_o marked in plot. Separation between the newly formed split states is $2 \times \alpha_o$	18

- 2.2 (a) 2-D and 3-D plot of Coulomb potential for bent water molecule with large peak due to potential of Oxygen atom and small peaks due to potential of Hydrogen atom. (b) Split states potential energy surface of zeroth order KH potential for bent geometry in presence of laser with polarization direction perpendicular to dipole with laser $\alpha_o = 3 a.u.$. The electronic potential for individual atom gets split into two. The lobes shown dichotomic behavior of split states. (c) Split states potential energy surface of zeroth order KH potential for bent geometry in presence of laser with polarization direction along the dipole with laser parameter $\alpha_o = 3 a.u.$. The electronic potential for individual atom gets split into two. The lobes shown dichotomic behavior of split states. (d) Split states potential energy surface of zeroth order KH potential for linear geometry in presence of laser with polarization direction along O-H bond axis with laser $\alpha_o = 3 a.u.$. The electronic potential for individual atom gets split into two. The lobes shown dichotomic behavior of split states. 19
- 2.3 (a) HF ground state energy using coemd-4 basis set of bent(blue plot) and linear(red plot) in KH frame in presence of laser with polarization direction perpendicular to dipole of bent water molecule and along the O-H axis for linear geometry with varying laser parameter α_o . At $\alpha_o > 0.151 a.u.$ linear geometry stabilizes over the bent geometry. (b) (a) HF ground state energy using coemd-4 basis set of bent(blue plot) and linear(red plot) in KH frame in presence of laser with polarization direction along the dipole of bent water molecule and perpendicular to the O-H axis for linear geometry with varying laser parameter α_o . At range of α_o , $0.132 a.u. < \alpha_o < 0.264 a.u.$ linear geometry stabilizes over the bent geometry but on increasing α_o beyond $0.264 a.u.$ the linear geometry destabilizes over bent geometry. 21
- 2.4 The 1-D potential energy space curve for varying H-O-H angle in presence of laser with $\alpha_o = 4 \text{ \AA}$ with direction perpendicular to dipole for bent geometry of water molecule calculated in KH frame using HF method and coemd-4 basis. The linear geometry which was a transition state without the laser has now become the equilibrium geometry in presence of linearly polarized laser and the bent geometry has been destabilized. 22
- 2.5 (a) Walsh diagram for water molecule. Most of the molecular orbitals are stabilized in bent geometry, therefore bent geometry is equilibrium geometry. Symmetries and orbital pictures have been shown in the plot. (b) Walsh diagram for water molecule in presence of the field with laser polarization direction perpendicular to dipole of bent water molecule and along the O-H axis for linear geometry and $\alpha_o = 4 \text{ \AA}$. All the MO's for linear geometry are now stabilized over the MO's for bent geometry. Symmetries and orbital pictures have been shown in plot. 23

- 2.6 (a) Molecular orbital energy calculated using Hartree Fock method, coemd-4 basis using KH potential for bent with laser polarization direction perpendicular to dipole. (b) Molecular orbital energy calculated using Hartree Fock method, coemd-4 basis using KH potential for linear geometry with laser polarization direction along O-H axis, with respect to varying laser parameter α_o . At higher α_o MO's become degenerate. 24
- 2.7 (a) Electron density for bent geometry with laser in direction perpendicular to dipole with varying laser parameter α_o . The electron density gets smeared along the laser polarization direction and electron accumulate at new split state centers separated by $2 \times \alpha_o$. (b) Electron density for linear geometry with laser in direction along O-H axis with varying laser parameter α_o . The electron density gets smeared along the laser polarization direction and electron accumulate at new split state centers separated by $2 \times \alpha_o$ 25
- 3.1 Time dependent electronic dynamics using modified algorithm of (t,t') method of bent geometry(blue plot) and linear geometry(red plot) in sine² envelope pulse with CW region with laser polarization perpendicular to dipole of bent geometry and along the O-H axis for linear geometry. The field(black plot) used has wavelength of 431 nm and a peak intensity of $2.2464 \times 10^{14} W/cm^2$. The time averaged energy has also been marked for CW region of pulse. The linear geometry has been stabilized over bent geometry in CW region. The energy of the bent and linear geometry has remained below their respective ionization energy supporting the fact that no ionization will take place during the dynamics. 31
- 3.2 Time dependent electronic dynamics of some intermediate geometries(green plot) from bent to linear in sine² envelope pulse with CW region. The field(black plot) used has wavelength of 431 nm and an intensity of $2.2464 \times 10^{14} W/cm^2$. The energy of geometry with H-O-H angle 172.8°, 149.7°, 142.1° and 126.9° goes very high than their respective ionization potential depicting their instability in laser. 32
- 3.3 (a) Population of the ground and excited states for bent geometry. The red plot is the population for ground state and is highly populated during the dynamics. The black curve is the electric field with field strengths marked. The red plot is the population for ground state while the other plots are the excited states population. The population of some excited states increase during the dynamics after around 20 a.u. while ground state population declines. (b) Population of the ground and excited states for linear geometry. The red plot is the population for ground state while the other plots are the excited states population. 33

Abbreviations

2-D	two-dimension
3-D	three-dimension
a.u.	atomic units
CIS	Configuration Interaction Singles
COEMD	Completeness Optimized Electron Momentum Density
CW	Continuous Wave
HF	Hartree Fock
KH	Kramers-Henneberger
MO	Molecular Orbital(s)
TDSE	Time Dependent Schrödinger Equation

Physical Constants

Speed of Light	c	$=$	$2.99792458 \times 10^8 \text{ ms}^{-2}$	(exact)
Electron rest mass	m	$=$	$9.10938291 \times 10^{-31} \text{ kg}$	
Mass of proton	m_p	$=$	$6.62507015 \times 10^{-34} \text{ kg}$	
Electron charge	e	$=$	$1.60217657 \times 10^{-19} \text{ C}$	
Plank's constant	h	$=$	$6.62507015 \times 10^{-34} \text{ J s}$	
Pi	π	$=$	3.1415926535897932	(upto double precision)

Symbols

α_0	Classical quiver distance	m
ω	Angular frequency	rads ⁻¹
E_0	Electric field strength	N/C
\hbar	Reduced Plank's constant	J s
i	Iota	
\vec{A}	Vector potential	
\AA	Angstrom	

Abstract

The work presented in this thesis addresses the possibility of trapping water molecule in a linear geometry in the presence of high-frequency, high-intensity electromagnetic radiation. **Chapter 1** of the thesis starts with a basic review of the literature, giving a description of Multiphoton ionization, Above-threshold ionization, Tunnel ionization and Higher harmonic generation in strong field interactions in molecules, together with a motivation of the problem. In **Chapter 2**, the reason for the question is analyzed. Using solutions of time independent Schrödinger equation in the oscillating frame of reference, it is shown that a linear geometry of water molecule is favoured over the bent geometry. The reason for this stabilization is then analyzed in terms of Kramers-Henneberger(KH) potential and orbital interactions as a function of laser parameters and geometry. Using Hartree Fock and Configuration Interaction Singles calculations at a converged all electron basis set, it is found that the stabilization of the linear geometry is 23.89 eV. In **Chapter 3**, time dependent calculations using a modified (t, t') method has been done in presence of electric field with aforementioned laser parameters in a \sin^2 envelope with the Continuous Wave region in between the rise and fall of pulse. Electronic wavepacket dynamics of water molecule is done with a realistic laser pulse of peak intensity $2.2464 \times 10^{14} \text{ W/cm}^2$ and frequency of 431 nm. The time average of the energy over the Continuous Wave region of the pulse is found to be lesser for the linear geometry indicating its stabilization. In contrast to 800 nm and a similar intensity giving ionization, in the off resonant 431 nm pulse with a rise time of 0.96 fs and pulse duration of 2.88 fs the stabilization is achieved and maintained.

Chapter 1

Introduction

1.1 Atoms and molecules in a strong laser

The interaction of light with quantum matter made of atoms and molecules has received much attention, both from experimentalists and theoreticians since the last few decades. The phenomena associated with light-matter interactions change as the laser intensity is increased. For a very long time, effects such as single photon absorption, electronic excitation and photo-ionization have been well studied when light with very low intensities interacts with atoms and molecules. The photons absorbed by atoms and molecules are resonant with excited energy levels or continuum state leading to excitation or photo-ionization.

Later in 1970's, as the laser intensities were further increased reaching the order of 10^{11} - 10^{14} W/cm², the usual perturbative treatment of light with atoms became inadequate because the field strengths at these high intensities were comparable to the internal electric fields of atoms and molecules. Therefore, non-perturbative electronic dynamics such as multi-photon ionization, above-threshold ionization, tunnel ionization[1, 2] and higher-order harmonic generation (HHG)[3, 4] were new phenomena that emerged.

Multi-Photon Ionization (MPI) is a process in which the electron absorbs multiple photons each of energy less than the atomic ionization potential from the intense

laser field to undergo ionization.[5] In MPI, the electrons absorbed only the minimum number of photons required for it to ionize and escape the parent atom. This could not explain the presence of *periodic oscillations* in the photo-electron spectra, since the electrons were found to absorb more photons than what was required for them to ionize and escape the atom in the case of Xenon atom.[6] This phenomenon of electrons absorbing more than the required number of photons for ionization was termed as *Above-Threshold Ionization(ATI)*. The difference between MPI and ATI is in the number of photons absorbed for ionization. While in MPI, the absorbed photons energy is equal to the ionization potential of the atom, in ATI more number of photons are absorbed to ionize the atom.

If the field strength is further increased, it can change the Coulombic potential felt by electron leading to barrier suppression in the laser polarization direction. At particular parameters, this suppressed barrier may lead to tunneling electrons which dominates the ionization process. This is termed as tunnel ionization. If the barrier is suppressed further the initially bound electron becomes a metastable state with energy above the barrier from one side and can escape from the potential. This is termed as *Over-the-Barrier Ionization (OTBI) or Above-Barrier Ionization(ABI) or Barrier-Suppression Ionization*. A quantitative picture of the mechanism can be derived using Keldysh parameter[7] which decides whether the system will tunnel ionize or ionize from above the barrier.

In all the effects above, the state of the electron after it gets ionized is unclear. One could think of possibilities of the electron, which is ionized, leaving the parent ion or remaining in the field oscillating in the laser polarization direction. The recollision model proposed by Corkum[8] is based on a classical picture which states that the electron oscillates in the field after getting tunnel-ionized and then can combine with the parent ion during the oscillation. This can lead to a recombination with the parent ion or can stimulate ionization or excitation of inner-electrons by collision. The three step model given by Corkum[8] states that, first the electron tunnel-ionizes, then accelerates in the field and after which it recombines with the parent ion. The recombination leads to the generation of photons at higher order multiples of the carrier frequency. This process is called *Higher Harmonic*

Generation. The first spectra was recorded [9] in 1987 by A. McPherson.

As the laser technology advanced, the lasers became ultra-fast and ultra-strong, the consequence of which being not only an intensity increase but also an increase in stable duration of the laser pulse from pico-seconds to femto-second and now atto-seconds using HHG.[10]

In 2000's, apart from the usual intuition of ionization of molecules in presence of laser in the high frequency regime. *stabilization* of atoms and molecules in presence of very high laser field strength has been proposed. When a strong field laser is shined on an atom or molecule the Coulombic potential combined with the intense fields interacts to create a new effective binding potential. The electrons become free from the Coulombic forces and they oscillate with the laser field. At very high frequencies and intensities the perturbative treatment of light with the atom becomes inconvenient because of strong electromagnetic forces becoming comparable to the nuclear binding potential experienced by the electron. A reformulation of the problem consisting of a transformation to an accelerated frame of reference called as the *Kramers-Henneberger(KH)* frame of reference has given a better understanding to the problem.[11]

New discrete bound states are formed. The new system -the laser-dressed atom, is thus stable against ionization. Theoretical calculations have shown an increase in lifetime of atomic Hydrogen in high intensity of circularly polarized laser.[12] This KH state has been realized for Hydrogen atom in linearly polarized laser where a dichotomy behavior in its orbitals is found as the laser parameters are varied.[13] The dichotomy behavior refers to the splitting of the initial Coulomb potential into two such that it looks as if there are now two nuclei rather than one. The idea of a KH atom is not just left in theoretical realm, signatures of stabilized atoms have been found experimentally in intense fields. Acceleration of neutral Helium atoms in their metastable states, as opposed to ionization have been found in intense short-pulse linearly polarized laser with intensity of order of $10^{15}\text{W}/\text{cm}^2$. [14] KH atom has been imaged using photoelectron spectra for Potassium atom in linearly polarized light with intensity of order of $10^{13}\text{W}/\text{cm}^2$. [15]

The next section describes the semi-classical treatment of Hamiltonian for an atom

in presence of electromagnetic field and its transformation to the KH frame of reference.

1.2 Kramers-Henneberger atom

The interaction of hydrogen atom, a one electron system, with an external classical electromagnetic field can be written in the form of a non-relativistic Hamiltonian within the Born-Oppenheimer approximation as:

$$\frac{1}{2m} \left[\frac{\hbar}{i} \vec{\nabla} - \frac{e}{c} \vec{A}(\vec{r}, t) \right]^2 \psi(\vec{r}, t) - e\Phi(\vec{r}, t)\psi(\vec{r}, t) + V(\vec{r})\psi(\vec{r}, t) = i\hbar \frac{\partial \psi}{\partial t}(\vec{r}, t) \quad (1.1)$$

Here, $\frac{\hbar}{i} \vec{\nabla}$ is the momentum operator, $\vec{A}(\vec{r}, t)$ and $\Phi(\vec{r}, t)$ are the vector and scalar potentials respectively. Here, $V(\vec{r})$ is the potential term comprising of an electron-nucleus attraction potential and $\psi(\vec{r}, t)$ represents the wave function for an electron. The electric field $\vec{E}(\vec{r}, t)$ and magnetic field $\vec{B}(\vec{r}, t)$ can be written in terms of the scalar and vector fields [16] as:

$$\vec{E}(\vec{r}, t) = -\vec{\nabla}\Phi(\vec{r}, t) - \frac{\partial \vec{A}(\vec{r}, t)}{\partial t} \quad (1.2)$$

$$\vec{B}(\vec{r}, t) = \vec{\nabla} \times \vec{A}(\vec{r}, t) \quad (1.3)$$

The fields \vec{E} and \vec{B} are invariant under the classical gauge transformation. On doing gauge transformation: $A \rightarrow \vec{A}' = \vec{A} + \vec{\nabla}\chi$, $\Phi \rightarrow \Phi' = \Phi - \partial_t \chi$, and introducing phase change to the wave function $\psi' = e^{-i\chi}\psi$, one can see that the Hamiltonian in Eq. [1.1] can be rewritten as:

$$\frac{1}{2m} \left[\frac{\hbar}{i} \vec{\nabla} - \frac{e}{c} \vec{A}(\vec{r}, t) \right]^2 \psi(\vec{r}, t) - e\Phi(\vec{r}, t)\psi(\vec{r}, t) + V(\vec{r})\psi(\vec{r}, t) = i\hbar \frac{\partial \psi}{\partial t}(\vec{r}, t) \quad (1.4)$$

One can see that the Hamiltonian remains invariant even after gauge transforming the vector and scalar potentials. Since only a phase change is introduced to the wave function, it remains unchanged.

In regions far from electrical charges the scalar potential can be taken to zero,

called the radiation gauge. Therefore, $\Phi = 0$ and \mathbf{A} is chosen such that $\vec{\nabla} \cdot \vec{A} = 0$ which is the Coulomb gauge condition. Thus, the applied electric field can be written as: $\vec{E}(t) = -\frac{d\vec{A}(t)}{dt}$. By taking these gauge transformations one can write the semi-classical Hamiltonian in Eq. [1.1] in a much simpler version which looks similar to TDSE.

For a typical linearly polarized light polarized along Z-direction in the lab frame, the vector potential is given by:

$$A(\vec{r}, t) = A_o \hat{z} \sin(\omega t - \vec{k} \cdot \vec{r}), \quad A_o = -E_o/\omega \quad (1.5)$$

where, E_o is the peak electric field strength, ω is the frequency of light used, k is the angular wavenumber given as $2\pi/\lambda \hat{n}$, \hat{n} being along the propagation direction and \vec{r} being the position vector. In general, the wavelength of light used is very large compared to the size of an atom and therefore, the $\vec{k} \cdot \vec{r}$ term is much less than 1 and thus can be dropped to get $A(\vec{r}, t) = A(t) = A_o \hat{z} \sin(\omega t)$ which is spatially independent. This is known as the *Dipole approximation*.

Using the Coulomb gauge condition and dipole approximation one can re-write the Hamiltonian for an Hydrogen atom in presence of an electric field as:

$$\frac{1}{2m} \left[\frac{\hbar}{i} \vec{\nabla} - \frac{e}{c} \vec{A}(t) \right]^2 \psi(\vec{r}, t) + V(\vec{r}) \psi(\vec{r}, t) = i\hbar \frac{\partial \psi}{\partial t}(\vec{r}, t) \quad (1.6)$$

Or,

$$\left[-\frac{\hbar^2}{2m} \vec{\nabla}^2 + \frac{e^2}{2mc^2} \vec{A}(t)^2 + \frac{i\hbar e}{mc} \vec{\nabla} \cdot \vec{A}(t) \right] \psi(\vec{r}, t) + V(\vec{r}) \psi(\vec{r}, t) = i\hbar \frac{\partial \psi}{\partial t}(\vec{r}, t) \quad (1.7)$$

The Eq. [1.7] is a look-alike of a TDSE if the second and the third term can be removed. To do this we introduce a unitary transformation to the wave function:

$$\Psi_{KH}(\vec{r}, t) = \hat{\Theta} \psi(\vec{r}, t) \quad (1.8)$$

where the Unitary operator is given by:

$$\hat{\Theta} = \exp\left\{ \frac{i}{\hbar} \int \left[\frac{i\hbar e}{mc} \vec{A}(t) \cdot \vec{\nabla} + \frac{e^2}{2mc^2} \vec{A}^2(t) \right] dt \right\} \quad (1.9)$$

$\Psi_{KH}(\vec{r}, t)$ is the wave function in a new frame of reference named as the Kramers-Henneberger frame of reference. Applying this transformation in Eq. [1.6], we get:

$$\frac{1}{2m} \left[\frac{\hbar}{i} \vec{\nabla} - \frac{e}{c} \vec{A}(t) \right]^2 \hat{\Theta}^\dagger \Psi_{KH}(\vec{r}, t) + V(\vec{r}) \hat{\Theta}^\dagger \Psi_{KH}(\vec{r}, t) = i\hbar \frac{\partial \hat{\Theta}^\dagger \Psi_{KH}(\vec{r}, t)}{\partial t} \quad (1.10)$$

On solving the right hand side of Eq. [1.10] one gets:

$$\left[\frac{-\hbar^2}{2m} \vec{\nabla}^2 \hat{\Theta}^\dagger + V(\vec{r}) \hat{\Theta}^\dagger \right] \Psi_{KH} = i\hbar \hat{\Theta}^\dagger \frac{\partial \Psi_{KH}}{\partial t} \quad (1.11)$$

Let,

$$\hat{H}_{ini} = \left[\frac{-\hbar^2}{2m} \vec{\nabla}^2 \hat{\Theta}^\dagger + V(\vec{r}) \hat{\Theta}^\dagger \right] \quad (1.12)$$

Applying transformation to \hat{H}_{ini}

$$\hat{H}_{KH} = \hat{\Theta} \hat{H}_{ini} \quad (1.13)$$

Using the Baker-Hausdorff-Campbell[17] formula to \hat{H}_{KH} :

$$e^{\hat{X}} \cdot \hat{Y} \cdot e^{-\hat{X}} = \hat{Y} + [\hat{X}, \hat{Y}] + \frac{1}{2!} [\hat{X}, [\hat{X}, \hat{Y}]] + \dots \quad (1.14)$$

We get:

$$\hat{H}_{KH} = \left[\frac{-\hbar^2}{2m} \vec{\nabla}^2 + V(\vec{r} + \vec{\alpha}(t)) \right] \quad (1.15)$$

where the time dependent potential is the Kramer-Henneberger potential and

$$\vec{\alpha}(t) = - \int \frac{e}{mc} \vec{A}(t) dt \quad (1.16)$$

For lasers, generally, the time dependent electric field is given by:

$$\vec{\alpha}(t) = \vec{\alpha}_0 \sin(\omega t)$$

Now that we have transformed the Hamiltonian as well as the wave function, it is

viable to write:

$$\hat{H}_{KH}\Psi_{KH} = \left[\frac{-\hbar^2}{2m} \vec{\nabla}^2 + V(\vec{r} + \vec{\alpha}_o \sin(\omega t)) \right] \Psi_{KH} = i\hbar \frac{\partial \Psi_{KH}}{\partial t} \quad (1.17)$$

This transformation has been done without any approximation to Eq. [1.6]. Eq. [1.17] looks similar to a TDSE except that the Hamiltonian is time dependent as can be seen from the potential term. The semi-classical Hamiltonian in Eq. [1.6] is now written in an accelerated electronic frame of reference from a laboratory frame of reference. This frame transformation is helpful in converting the TDSE into a time independent Schrödinger equation discussed later in this thesis.

The current work looks at the states of water molecule in the KH frame and develops an understanding of its dynamics. The next section, therefore describes the electronic structure of water molecule.

1.3 Water molecule- Geometry and electronic structure

The experimental geometry for water molecule in its gas phase has been found with O-H length 0.957 Å, H-O-H angle to be 104.47° [18] as compared to MP2 calculations showing O-H bond length to be 0.957 Å and H-O-H angle to be 104.2°. The geometry for water molecule can be explained using the Valence Shell Electron Pair Repulsion (VSEPR) theory.[19] The Oxygen with two bond pairs and two lone pairs make the hybridization of water molecule to be sp^3 which gives a tetrahedral geometry with bond angles to be 109.5°. But the lone pair-lone pair repulsion being more than the lone pair-bond-pair repulsion, the lone pairs push the bond pairs even more and hence the bond angle becomes 104.2° as shown in Fig.(1.1). Another explanation for the equilibrium geometry to be bent for water molecule can be given through Walsh diagram.[20] By looking at the Molecular Orbitals for bent and linear water molecule, one can see that most of the MO's are stabilized in the bent geometry. The Walsh diagram is discussed in details in the second chapter of this thesis. Therefore, water is bent in equilibrium geometry as shown

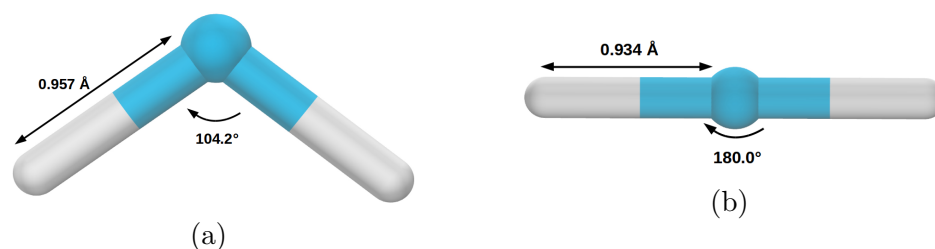


FIGURE 1.1: (a) Equilibrium geometry for water molecule with angles and distances marked in figure, computed with geometry optimization using Moller-Plesset(second) order(MP2) method with coemd-ref basis set. MP2 energy is -76.06689 Hartree (b) Optimized linear geometry for water molecule with angles and distances marked in figure, computed using Moller-Plesset(second) order(MP2) method and coemd-ref basis set, MP2 energy is -76.01557 Hartree.

in Fig.(1.1a). There is another geometry of water molecule as a transition state which is linear in fashion shown in Fig.(1.1b) optimized using MP2 method and coemd-ref basis.[21]

By calculating the 1-D potential energy surface for bent to linear transition, the energy difference between the linear and bent water was found to be $1.394 eV$ shown in Fig.(1.2).

The CIS calculation for energies of the excited states for water molecule with the varying coordinates has also been computed as shown in Fig.(1.3) with the excitation energy marked in the plot for the bent geometry and matched with experimental data.[22] The frequency of light that should be used on the molecule should be non-resonant to any of the frequency for excitation. This will ensure that the molecule has been probed in its ground state without exciting or eventually exciting the molecule.

The ionization potential for water molecule in bent geometry is $11.12 eV$ calculated by computed ground state energy for H_2O^+ using MP2 method and coemd-ref basis.

1.4 Objectives and Overview

The absorption spectrum for water molecule shows a minimum in absorption at $418 nm$. [23] This implies that at this wavelength the transition dipoles for water

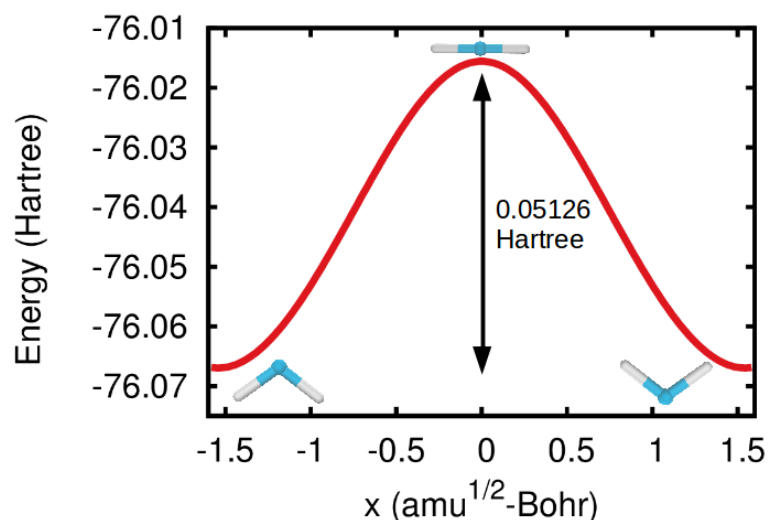


FIGURE 1.2: Barrier for water inversion for H-O-H angle variation from bent to linear geometry computed using MP2 method and coemd-ref basis. The energy difference between the bent and linear geometry using MP2 method is 1.394 eV with equilibrium geometry being bent and transition state being linear.

molecule are minimum due to which molecule has the least chance of getting excited or ionized at this frequency. Therefore, intensity of light can be kept high at this frequency without bringing much destruction to the molecule. When the field reach the order of $10^{15} - 10^{16}$ W/cm², it exerts a force that is comparable to electron-nucleus Coulombic forces. Such strong fields trigger nuclear motion of atoms and molecules. Various phenomenon associated with nuclear motion apart from vibrational excitation have been found. Structural deformation like bond softening can occur.[25] Intense laser fields could cause sudden ionization, inter-nuclear potentials can become repulsive leading to Coulomb explosions and flying of molecular fragments.[26] Geometry modifications happen in molecules as they adapt themselves in the presence of high frequency and high intensity laser.[27] Experiments have shown the bent structure of CO₂ molecule as opposed to linear and linear structure of SO₂ molecule before dissociating in presence of laser.[28] Water molecule taken in an intense femtosecond laser pulse where the molecule is found linear followed by ionization and subsequent Coulomb explosion, have also been found experimentally using ion momentum imaging technique.[29] Results from this ion momentum imaging experiment shows O-H bond stretching in presence of field, alignment of H-H axis and laser polarization direction and increase

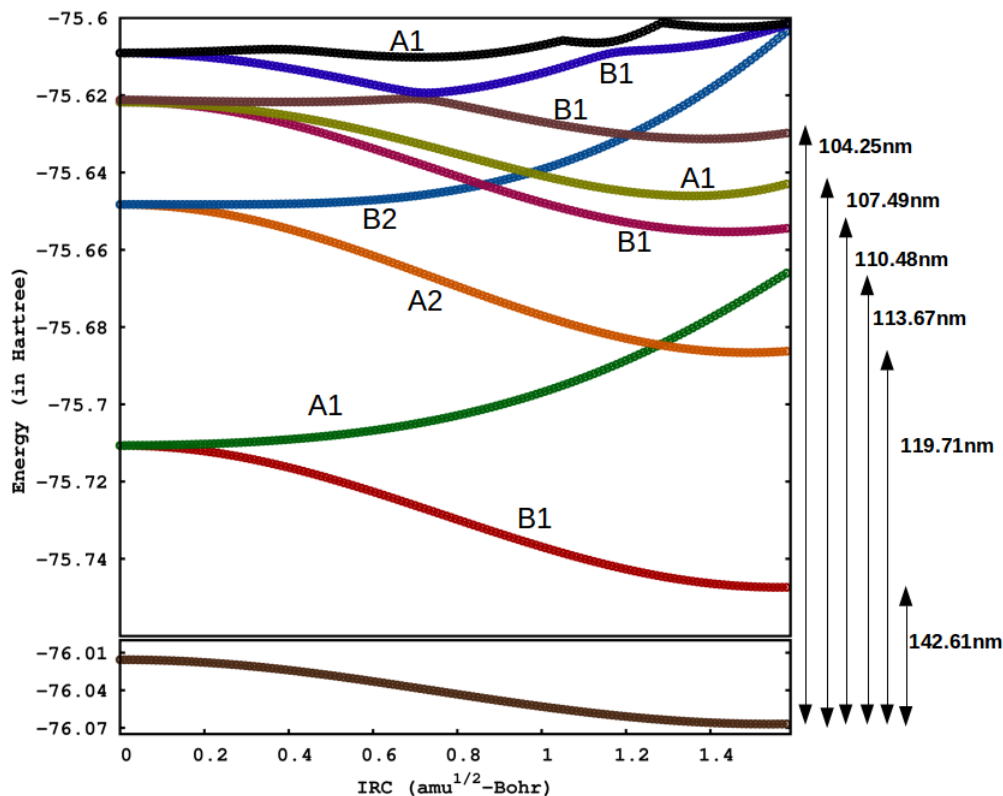


FIGURE 1.3: Excited states of intermediate geometries from bent to linear calculated using MP2 method and coemd-ref basis with varying coordinates from bent to linear geometry along with the ground state energy(brown plot). The excitation energy for bent geometry has been marked in the plot.

in H-O-H angle with maximum probability at $140 - 180^\circ$. They concluded that water molecule is found to linearize prior to Coulomb explosion into its constituent ions in $790 \text{ nm}, 3 \times 10^{16} \text{ W/cm}^2$ laser. Our objective in the study is to mimic this straightening of water molecule but the intensity should be kept in such a way that the molecule does not ionize or get dissociated in presence of the field unlike the experimental indication.

The second Chapter of this thesis includes the electronic structure time independent calculation in the Kramers-Henneberger frame of reference with respect to the varying laser parameters. The KH nuclear potential for water molecule averaged over one pulse cycle is shown. The Walsh diagram for AH_2 kind of system gives the reasoning for the geometry of water molecule to be stabilized in bent fashion. The same has been computed in presence of the field which gives a better understanding of the stabilization of linear geometry. These calculations are a

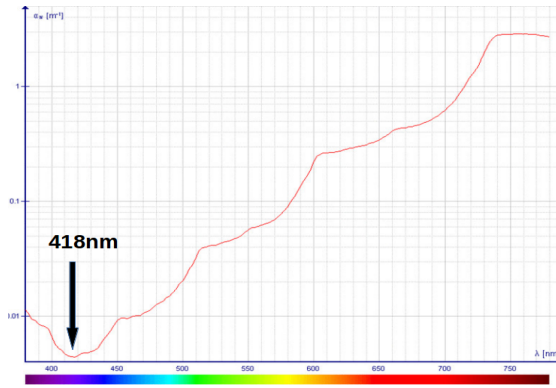


FIGURE 1.4: Absorption spectrum for water molecule in 400 – 700 nm range with a minimum in absorption at 418 nm . At this frequency, the transition dipoles are minimum and thus intensity can be cranked up at this frequency without destruction of molecule. Image taken from https://upload.wikimedia.org/wikipedia/commons/b/b5/Water_absorption_coefficient_large.gif

good motivation for observing the time dependent dynamics of the molecule as they provide estimate of laser parameters and reasons for the linearization of bent geometry.

The third Chapter deals with the time dependent electronic dynamics for bent and linear geometry of water in presence of sine² envelope with Continuous Wave(CW) region in between the rise and off time. We have used a modified algorithm for solving Time dependent Schrödinger using (t, t') method.[30]

The thesis ends with results and discussion of the work done along with summary and appendix including the codes and supplementary information used throughout the work.

References

- [1] S. L. Chin, F. Yergeau, and P. Lavigne, *J. Phys. B: At. Mol. Phys.* **18**, L213 (1985).
- [2] N. B. Delone and V. P. Krainov, *Multiphoton processes in Atoms*, Springer, Berlin, Heidelberg, 1994.
- [3] A. McPherson, G. Gibson, H. Jara, U. Johann, I.A. McIntyre, K. Boyer, and C.K. Rhodes, *J. Opt. Soc. Am. B* **4**, 595 (1987).
- [4] X. F. Li, A. L'Huillier, M. Ferray, L. A. Lompre, and G. Mainfray, *Phys. Rev. A* **39**, 5751 (1989).
- [5] S. Voronov and N. B. Delone, *Soviet Phys. JETP* **23**, 54 (1966).
- [6] P. Agostini, F. Fabre, G. Mainfray, G. Petite, and N. K. Rahman, *Phys. Rev. Lett.* **42**, 1127 (1979).
- [7] L. V. Keldysh, *Sov. Phys. JETP* **20**, 1307-1314 (1965).
- [8] P. B. Corkum, *Phys. Rev. Lett.* **71**, 1994 (1993).
- [9] A. McPherson, G. Gibson, H. Jara, U. Johann, T. S. Luk, I. A. McIntyre, K. Boyer, and C. K. Rhodes, *J. Opt. Soc. Am. B* **4**, 595 (1987).
- [10] M. Hentschel, R. Kienberger, C. Spielmann, G. A. Reider, N. Milosevic, T. Brabec, P. Corkum, U. Heinzmanns, M. Dreschers, and F. Krausz, *Nature* **414**, 509 (2001).
- [11] W. C. Henneberger, *Phys. Rev. Lett.* **21**, 838 (1968).

-
- [12] M. Pont and M. Gavrilu, *Phys. Rev. Lett.* **65**, 2362-2365 (1990).
- [13] M. Pont, N. R. Walet, M. Gavrilu, and C. W. McCurdy, *Phys. Rev. Lett.* **61**, 939 (1988).
- [14] U. Eichmann, A. Saenz, S. Eilzer, T. Nubbemeyer, and W. Sandner, *Phys. Rev. Lett.* **110**, 203002 (2013).
- [15] F. Morales, M. Richter, S. Patchkovskii, and O. Smirnova, *Proc. Natl. Acad. Sci.* **108**, 16906-16911 (2011).
- [16] D. J. Griffith, *Introduction to Electrodynamics*, Pearson Education Inc., New Jersey, USA, 2013.
- [17] F. Hausdorff, *Ber Verh Saechs Akad Wiss Leipzig* **58**, 19-48 (1906).
- [18] J. B. Hasted, *Liquid water: Dielectric properties, in Water A comprehensive treatise*, New York, USA, p. 255-309, Vol 1, 1972.
- [19] W. L. Jolly, *Modern Inorganic Chemistry*, McGraw-Hill, New York, USA, p. 77-90, 1984.
- [20] A. D. Walsh, *J. Chem. Soc.* **0**, 2260-226 (1953).
- [21] J. Lehtola, P. Manninen, M. Hakala, and K. Hämäläinen, *J. Chem. Phys.* **137**, 104105 (2012).
- [22] R. V. Harrevelt and M. C. V. Hemert, *J. Chem. Phys.* **112**, 5777 (2000).
- [23] R. M. Pope and E. S. Fry, *Applied Optics* **36**, 33 (1997).
- [24] U. Eichmann, T. Nubbemeyer, H. Rottke, and W. Sandner, *Nature* **461**, 1261-1264 (2009).
- [25] A. Zavriyev, H. G. Muller, and D. W. Schumacher, *Phys. Rev. Lett.* **64**, 1883. (1990).
- [26] J H Posthumus, A J Giles, M R Thompson, and K Codling, *Phys. B: At. Mol. Opt. Phys.* **29**, 5811-5829 (1996).

-
- [27] C. Cornaggia, F. Salin, and C. Le Blanc, *J. Phys. B: At. Mol. Opt. Phys.*, **29**, L749 (1996).
- [28] J. H. Sandersont, R. V. Thomas, W. A. Bryan, W. R. Newell, A. J. Langley, and P. F. Taday, *Phys. B: At. Mol. Opt. Phys.* **31**, L599-L606 (1998).
- [29] J. H. Sanderson, A. El-Zein, W. A. Bryan, W. R. Newell, A. J. Langley, and P. F. Taday, *Phys. Rev. A* **59**,R2567(R) (1999).
- [30] U. Peskin, and N. Moiseyev, *J. Chem. Phys.* **99**, 4590 (1993).

Chapter 2

Why water should linearize in a linearly polarized light?

The electronic structure for water molecule has been studied using the Hartree Fock method and coemd-4 basis [1] in the high frequency regime of Kramers-Henneberger(KH) frame of reference and time averaged physical properties have been computed. These calculations support the fact that linear geometry for water molecule should get stabilized than the bent geometry in presence of the field. These calculations also help us finding the laser polarization direction and the parameters of the laser to be used in actual time-dependent dynamics.

2.1 Split states

The KH hamiltonian for an atom followed from Eq. [1.17] is given by:

$$H_{KH}\Psi_{KH} = \left[\frac{-\hbar^2}{2m} \vec{\nabla}^2 + V(\vec{r} + \vec{\alpha}(t)) \right] \Psi_{KH} = i\hbar \frac{\partial \Psi_{KH}}{\partial t} \quad (2.1)$$

Extending this to molecules, the potential term will have nuclear-electron attraction term and an electron-electron repulsion term, given by:

$$V(\vec{r} + \vec{\alpha}) = \sum_{Ni} V_{Ne_i}(\vec{r} + \vec{\alpha}) + \sum_{ij, i < j} V_{e_i e_j}(\vec{r}),$$

where i, j are electron index and N is nucleus index.

As can be seen above, the transformation to an accelerated frame takes place only in the Nuclear-electron attraction term. This term can be further expanded using a Fourier expansion giving:

$$\sum_{Ni} V_{Ne_i}(\vec{r} + \vec{\alpha}) = V_o + \sum_{k=1}^{\infty} V_k \cos(k\omega t) + i \sum_{k=1}^{\infty} V'_k \sin(k\omega t),$$

where,

$$\begin{aligned} V_o &= \frac{1}{2\pi} \int_0^{2\pi} \sum_{Ni} V_{Ne}(\vec{r} + \vec{\alpha}_o \cos(\tau)) d\tau \\ V_k &= \frac{1}{2\pi} \int_0^{2\pi} \sum_{Ni} V_{Ne}(\vec{r} + \vec{\alpha}_o \cos(\tau)) \cos(n\tau) d\tau \\ V'_k &= \frac{1}{2\pi} \int_0^{2\pi} \sum_{Ni} V_{Ne}(\vec{r} + \vec{\alpha}_o \cos(\tau)) \sin(n\tau) d\tau. \end{aligned}$$

The sine term goes to zero in the integration. Therefore, we are left with only the cosine term in the expansion.

$$V_{Ne}(\vec{r} + \vec{\alpha}) = V_o + \sum_{k=1}^{\infty} \frac{1}{2\pi} \int_0^{2\pi} \sum_{Ni} V_{Ne}(\vec{r} + \vec{\alpha}_o \cos(\tau)) \cos(n\tau) d\tau \cos(k\omega t)$$

In the high frequency regime, the high order terms in the expression become very small as compared to the zeroth order term[2] and therefore can be neglected.

Thus, we can write the final Hamiltonian as:

$$H_{KH} = \left[\sum_i \frac{-\hbar^2}{2m} \vec{\nabla}_e^2 + \sum_{AB, A < B} V_{N_A N_B}(\vec{R}) + \frac{1}{2\pi} \int_0^{2\pi} \sum_{ni} V_{ne_i}(\vec{r} + \vec{\alpha}) d\tau + \sum_{ij, i < j} V_{e_i e_j}(\vec{r}) \right] \quad (2.2)$$

Since the Hamiltonian is time independent, separation of variables \vec{r} and t can be done to get a time independent eigenvalue problem of the form:

$$H_{KH}\Psi_{KH} = E_{KH}\Psi_{KH}$$

Furthermore, methods like Hartree-Fock and Configuration Interaction can be applied to such equations to get the eigenvalues and eigenfunctions for the molecule in presence of oscillating fields in the high frequency regime in Kramers-Henneberger frame.

The typical laser linearly polarized in the Z-direction that is used has the form:

$$\vec{E}(t) = \hat{z}E_0\cos(\omega t); \quad E_0 = \alpha_0\omega^2$$

The frequency of the laser is ω and the max field strength is E_0 . The intensity of laser is given by $I = \frac{1}{2}\epsilon_0|\vec{E}|^2c$, where c is the speed of light and ϵ_0 is the vacuum permittivity.

The electronic cloud in an oscillating temporal field of very high strengths, will oscillate with the field in the laboratory frame of reference. On going to the electronic frame of reference, the potential due to the nucleus can be seen to oscillate with the frequency and α_0 of the field. This frame is the Kramers-Henneberger frame of reference. One can compute the time averaged zeroth order KH potential to find that the original Coulombic potential shows a dichotomic behavior as if there are now two nucleus present rather than one. This frame-transformed potential gives rise to what are called the Split states in an atom which are separated by $2 \times \alpha_0$. The newly formed split potential will have its own bound states.

$$V_0 = \frac{1}{2\pi} \int_0^{2\pi} \sum_{Ni} V_{Ne}(\vec{r} + \vec{\alpha}_0\cos(\tau))d\tau \quad (2.3)$$

The split potential can be computed for molecules using Eq. [2.3]. The zeroth order KH potential for linear geometry water molecule is shown in Fig.(2.1). The black curve in the figure is the Coulomb potential without the field. As the laser parameter α_0 is increased the split states are formed and separate in distance of

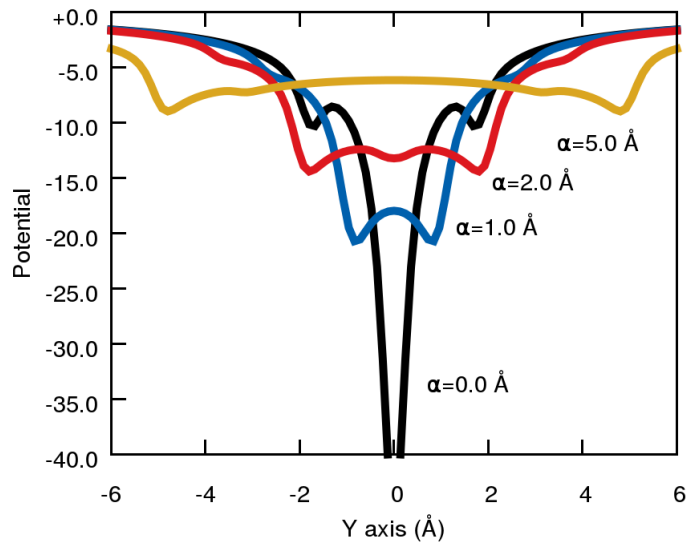


FIGURE 2.1: Coulomb potential(black curve) for linear geometry water molecule in presence of oscillating field with varying laser parameter α_o . Coulomb potential gets split into two as α_o is increased. Value of α_o marked in plot. Separation between the newly formed split states is $2 \times \alpha_o$.

$2 \times \alpha_o$ as if there are two nuclei rather than one. The potential energy surface for zeroth order KH potential has also been computed for bent geometry with and without the field as well as for the linear geometry water molecule shown in Fig.(2.2). As can be seen the potential without the field, it is the usual Coulomb potential concentrated on the atom centers. The 2-D plot shows a large peak for Oxygen atom and a small peak each for Hydrogen atom. As the laser is applied with polarization direction perpendicular to dipole and along the dipole of bent water molecule, the Coulomb potential gets split evenly on both sides of the Oxygen atom and Hydrogen atom with $2 \times \alpha_o$ separation along the laser polarization direction. Similarly for the linear geometry, when the laser is applied with polarization direction along the O-H axis the potential splits into two along the laser polarization direction.

In Fig.(2.2a), the 2-D plot of Coulomb potential for bent water molecule is shown. It has a larger peak due to potential of Oxygen atom and smaller peaks due to potential of Hydrogen atom. When laser is applied with polarization direction perpendicular to dipole with laser $\alpha_o = 3 a.u.$, the electronic potential for individual atom gets split into two. As can be seen in the Fig.(2.2b), new lobes that are formed in presence of the laser showing dichotomic behavior of split

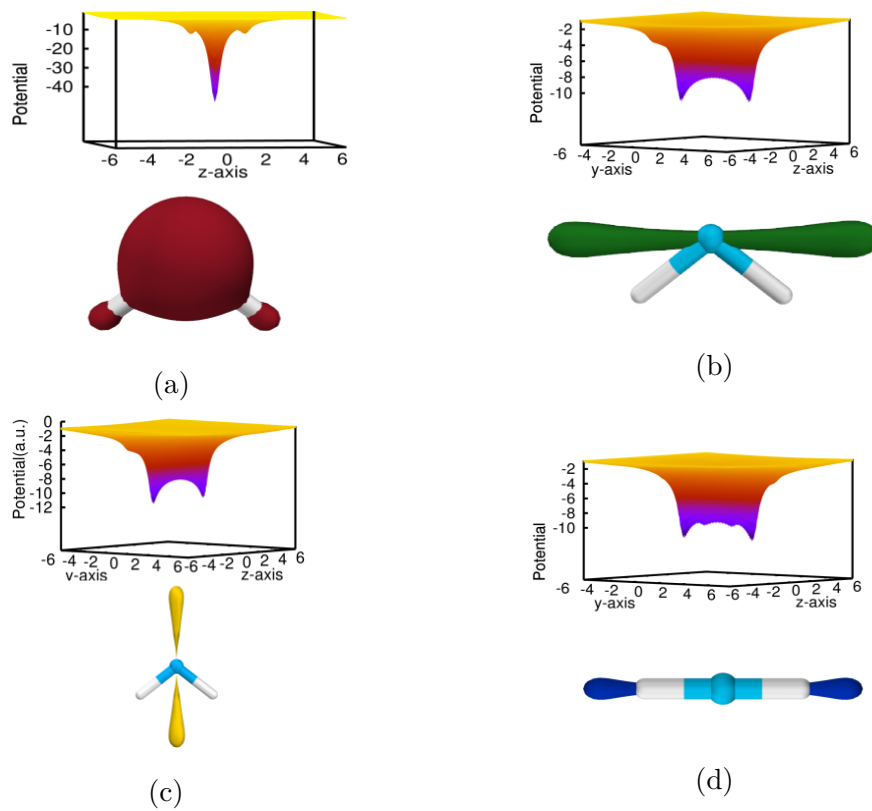


FIGURE 2.2: (a) 2-D and 3-D plot of Coulomb potential for bent water molecule with large peak due to potential of Oxygen atom and small peaks due to potential of Hydrogen atom. (b) Split states potential energy surface of zeroth order KH potential for bent geometry in presence of laser with polarization direction perpendicular to dipole with laser $\alpha_o = 3 a.u.$. The electronic potential for individual atom gets split into two. The lobes shown dichotomic behavior of split states. (c) Split states potential energy surface of zeroth order KH potential for bent geometry in presence of laser with polarization direction along the dipole with laser parameter $\alpha_o = 3 a.u.$. The electronic potential for individual atom gets split into two. The lobes shown dichotomic behavior of split states. (d) Split states potential energy surface of zeroth order KH potential for linear geometry in presence of laser with polarization direction along O-H bond axis with laser $\alpha_o = 3 a.u.$. The electronic potential for individual atom gets split into two. The lobes shown dichotomic behavior of split states.

states. Fig.(2.2c) shows the split state potential energy surface for bent water with laser polarization direction along the dipole. The electronic potential gets split in direction of laser polarization direction with new lobes showing the dichotomic behavior. In Fig.(2.2d), split states potential energy surface of zeroth order KH potential for linear geometry water molecule in presence of laser with polarization direction along O-H bond axis with laser $\alpha_o = 3 a.u.$ is shown. Similar to bent water, the potential for individual atom gets split into two and the newly formed

lobes show the dichotomic behavior of the split states.

2.2 Electronic structure in presence of field

The Hartree Fock(HF) method and Configuration Interaction Singles(CIS) method has been used on Hamiltonian given by Eq. [2.2] with Kramers-Henneberger potential using coemd-4 basis set to compute the electronic structure for water molecule in linearly polarized light. The calculation has been done using KH approximation of very high-frequency of light and therefore only the zeroth order term is taken in the KH potential.

The HF ground state energy of bent and the linear geometry using coemd-4 basis set has been computed using KH potential with laser polarization direction perpendicular to dipole of bent geometry and along the O-H axis of linear geometry with varying laser parameter α_o as shown in Fig.(2.3a). One can see that while initially without laser the bent was more stable than linear but as α_o is increased, from $\alpha_o > 0.151a.u.$ the energy of the linear geometry becomes lower than the bent geometry. The energy separation is quite significant for $2a.u. < \alpha_o < 8a.u.$. Similar calculation has also been done but with different laser polarization direction as well. HF ground state energy of bent and the linear geometry using coemd-4 basis set has been computed using KH potential with laser polarization direction along the dipole for bent geometry and perpendicular to the O-H bond axis for linear geometry of water molecule. As can be seen in Fig.(2.3b), the linear geometry stabilizes over the bent geometry for a small range of α_o , given $0.132 a.u. < \alpha_o < 0.264 a.u.$. On increasing the α_o laser parameter, the bent geometry stabilizes again in the laser field over the linear geometry. The basis set used is the standard basis set available on the EMSL basis set library. The electron density in water molecule is present mostly on the Oxygen atom due to its high electronegativity and thus the Hydrogens are delta positively charged. The dichotomic behavior of the Oxygen and Hydrogen atom can be seen in electronic potential in presence of the field as shown in Fig.(2.2). One would expect the delta positive Hydrogen atoms to be attracted towards the newly formed lobes and thus

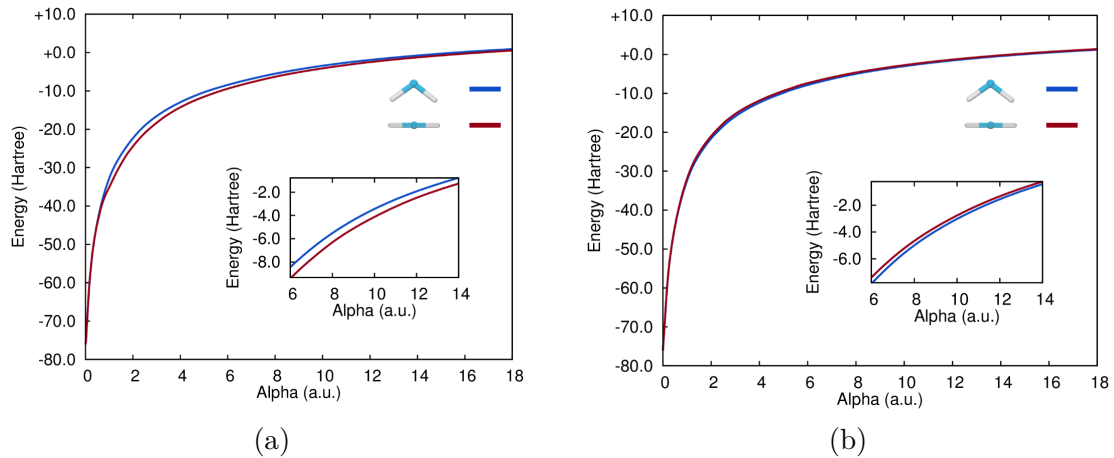


FIGURE 2.3: (a) HF ground state energy using coemd-4 basis set of bent (blue plot) and linear (red plot) in KH frame in presence of laser with polarization direction perpendicular to dipole of bent water molecule and along the O-H axis for linear geometry with varying laser parameter α_o . At $\alpha_o > 0.151 \text{ a.u.}$ linear geometry stabilizes over the bent geometry. (b) (a) HF ground state energy using coemd-4 basis set of bent (blue plot) and linear (red plot) in KH frame in presence of laser with polarization direction along the dipole of bent water molecule and perpendicular to the O-H axis for linear geometry with varying laser parameter α_o . At range of α_o , $0.132 \text{ a.u.} < \alpha_o < 0.264 \text{ a.u.}$ linear geometry stabilizes over the bent geometry but on increasing α_o beyond 0.264 a.u. the linear geometry destabilizes over bent geometry.

the linear structure of water should get stabilized in presence of the field. For the direction of laser polarization along the dipole for water molecule, the Hydrogen atoms will be attracted equally towards both the newly formed split state lobes shown in Fig.(2.2c) due to which they will try to remain stabilize in the middle such that the Hydrogens and Oxygen fall on a single line making the linear geometry stabilized in this laser polarization direction as well. But the HF calculations shown in Fig.(2.3) show that the direction of the electric field should be such that it is perpendicular to the dipole for bent geometry water molecule to favor the stabilization over a large range of α_o . Due to which the calculation hereafter are all done with the favored polarization direction perpendicular to the dipole of bent water and along the O-H axis of the linear geometry of water molecule.

The HF ground state energy has been computed with varying coordinates from bent to linear transition in KH frame averaged over one pulse cycle with direction of polarization of light taken in direction perpendicular to dipole for bent geometry water molecule. The linear geometry has now been found to become a minima as

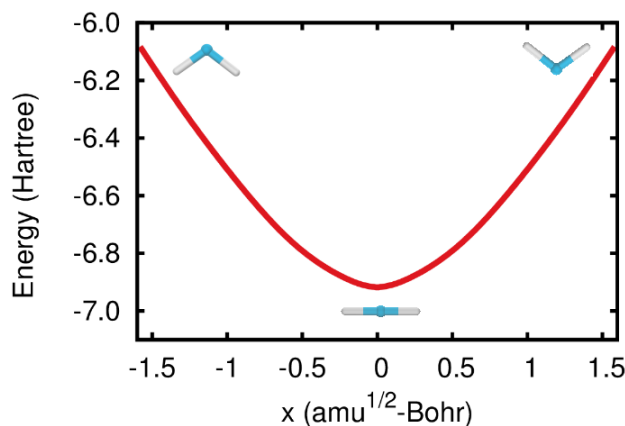


FIGURE 2.4: The 1-D potential energy space curve for varying H-O-H angle in presence of laser with $\alpha_0 = 4 \text{ \AA}$ with direction perpendicular to dipole for bent geometry of water molecule calculated in KH frame using HF method and coemd-4 basis. The linear geometry which was a transition state without the laser has now become the equilibrium geometry in presence of linearly polarized laser and the bent geometry has been destabilized.

shown in Fig.(2.4), thus stabilization over the top of the barrier has been obtained while the bent geometry now destabilized in presence of the field.

The stability of bent geometry over linear geometry for water can be rationalized using the orbital pictures in the Walsh diagram.[3] The diagram represents the qualitative picture of the Molecular orbitals along the coordinates.

From the Fig.(2.5a) , with the state symmetries marked, one can see that most of the orbitals are stabilized for bent geometry without the laser. This is the reason why equilibrium geometry of water has is found in bent fashion. The Walsh diagram for water molecule has been computed in presence of the field as shown in Fig.(2.5b) with HF method and coemd-4 basis. The energy of the MO has been plotted with respect to varying coordinates for intermediate geometries from bent to linear. The new plot obtained has all the molecular orbitals for linear geometry stabilized over the orbitals of bent geometry. Therefore, we can expect the molecule to linearize in presence of the field. The direction of polarization of light is taken to be perpendicular to the dipole for bent geometry water molecule. The energy of MO using HF method and coemd-4 basis has been computed in presence of laser with polarization direction perpendicular to dipole for bent geometry and parallel to O-H bond axis in linear geometry with respect to varying

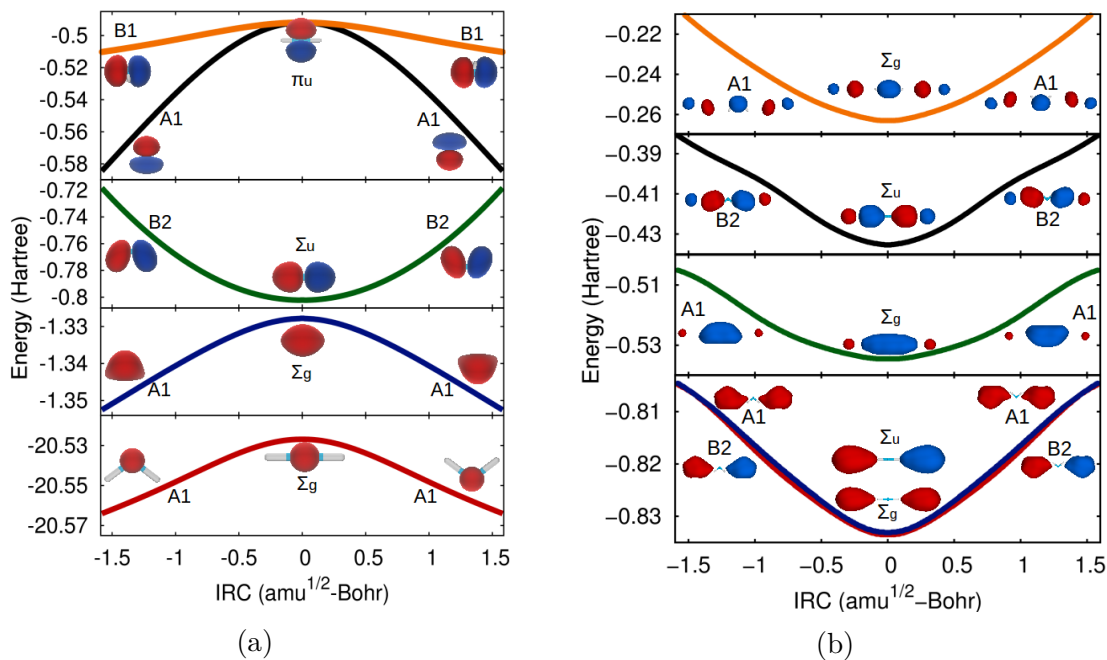


FIGURE 2.5: (a) Walsh diagram for water molecule. Most of the molecular orbitals are stabilized in bent geometry, therefore bent geometry is equilibrium geometry. Symmetries and orbital pictures have been shown in the plot. (b) Walsh diagram for water molecule in presence of the field with laser polarization direction perpendicular to dipole of bent water molecule and along the O-H axis for linear geometry and $\alpha_o = 4 \text{ \AA}$. All the MO's for linear geometry are now stabilized over the MO's for bent geometry. Symmetries and orbital pictures have been shown in plot.

laser parameter α_o as shown in Fig.(2.6). It can be seen that all the MO at very large α_o becomes nearly degenerate but still the energy of the orbitals remain negative. Electron density computed using HF method and coemd-4 basis for both linear and bent geometry with respect to varying α_o has been plotted with laser polarization direction perpendicular to dipole of bent geometry and parallel to O-H axis of linear geometry as shown in Fig.(2.7). As the laser parameter α_o is increased, the electron density gets concentrated near the newly formed sites of split states as discussed in first section of this chapter. The electron density gets smeared from the atom center in the laser polarization direction as can be seen on increasing the isovalue. The separation between the newly formed split state center is $2 \times \alpha_o$

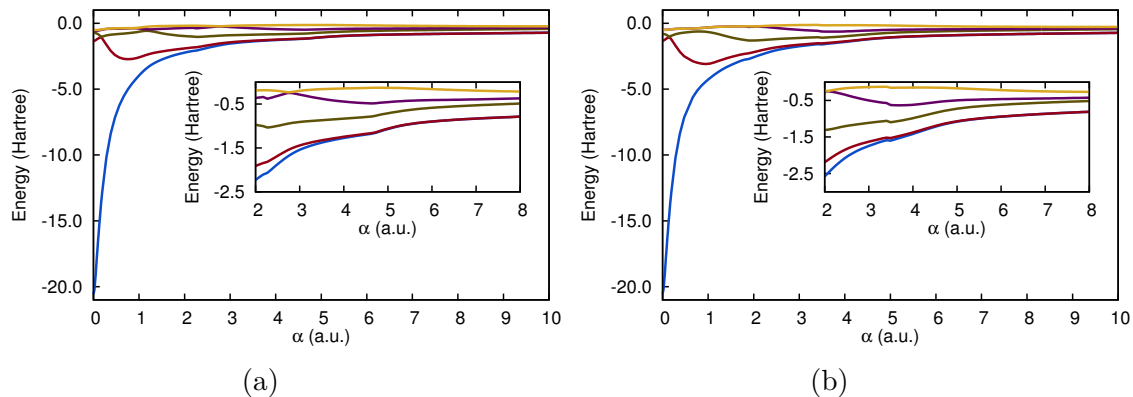


FIGURE 2.6: (a) Molecular orbital energy calculated using Hartree Fock method, coemd-4 basis using KH potential for bent with laser polarization direction perpendicular to dipole. (b) Molecular orbital energy calculated using Hartree Fock method, coemd-4 basis using KH potential for linear geometry with laser polarization direction along O-H axis, with respect to varying laser parameter α_o . At higher α_o MO's become degenerate.

2.3 Conclusion

The HF calculation using KH potential on both linear and bent as well as the intermediate geometry provides a good estimate of the laser parameters and laser polarization direction. The stability of linear geometry in KH frame is applicable to high-frequency regime of electromagnetic spectrum and at $\alpha_o > 0.151 a.u.$. With these parameters, one can perform the time dependent calculation on the bent, linear, and the intermediate geometries using a high-frequency laser. The energy separation between the bent and the linear geometry in KH calculation is significant for α_o between $2 a.u.$ to $8 a.u.$ and therefore any α_o between $2 a.u.$ to $8 a.u.$ can be chosen. The direction of laser polarization in which the stabilization can be achieved is perpendicular to the dipole of bent water molecule and parallel to the O-H bond axis for linear water.

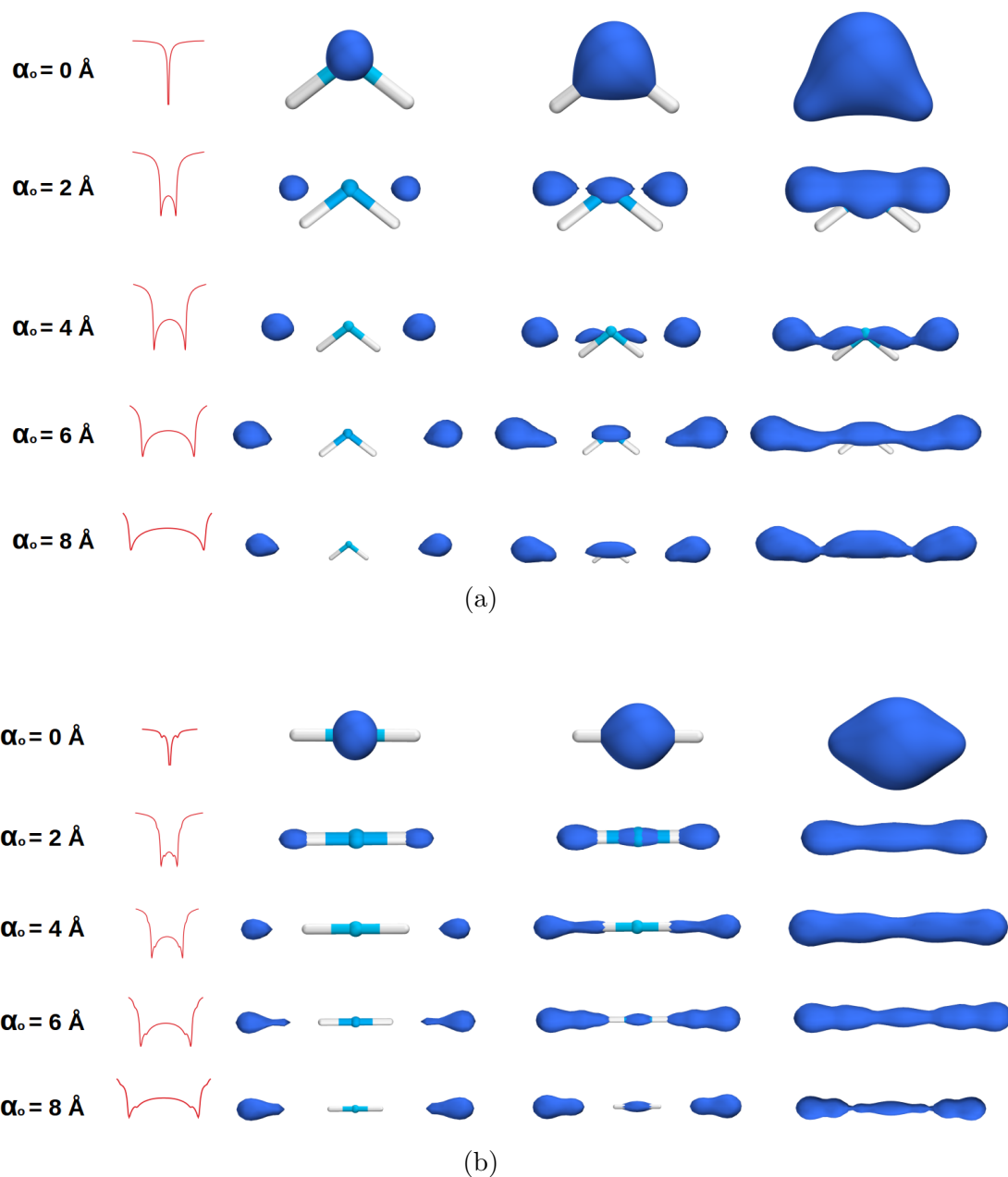


FIGURE 2.7: (a) Electron density for bent geometry with laser in direction perpendicular to dipole with varying laser parameter α_0 . The electron density gets smeared along the laser polarization direction and electron accumulate at new split state centers separated by $2 \times \alpha_0$. (b) Electron density for linear geometry with laser in direction along O-H axis with varying laser parameter α_0 . The electron density gets smeared along the laser polarization direction and electron accumulate at new split state centers separated by $2 \times \alpha_0$.

References

- [1] J. Lehtola, P. Manninen, M. Hakala, and K. *Hämäläinen*, *J. Chem. Phys.* **137**, 104105 (2012).
- [2] J. I. Gersten and M. H. Mittleman, *J. Phys. B: At. Mol. Phys.* **9**, 2561 (1976).
- [3] A. D. Walsh, *J. Chem. Soc.* **0**, 2260-226 (1953).
- [4] P. Balanarayan and N. Moiseyev, *Mol. Phys.* **111**, 1814-1822 (2013).
- [5] Q. Wei, Pi. Wang, S. Kais, D. Herschbach, *Chem. Phys. Lett.* **683**, 240 (2017).
- [6] P. Balanarayan and N. Moiseyev, *Phys. Rev. Lett.* **110**, 253001 (2013).
- [7] Q. Wei, S. Kais, and D. Herschbach, *J. Chem. Phys.* **129**, 21440 (2008).
- [8] Q. Wei, S. Kais, and N. Moiseyev, *Phys. Rev. A: At., Mol., Opt. Phys.* **76**, 13407 (2007).
- [9] P. Balanarayan and N. Moiseyev, *Phys. Rev. A: At., Mol., Opt. Phys.* **85**, 32516 (2012).

Chapter 3

Linearizing water molecule

The Kramers-Henneberger calculation has provided a good estimate of the direction and the laser parameters that can be used for the light. We have calculated the time dependent electronic dynamics of both the bent, linear geometry, and all the intermediate geometry in presence of a sine^2 envelope with 120 optical cycles, 120 *a.u.* duration with a Continuous Wave(CW) region of 40 *a.u.* duration in between the rise and fall of the laser using a modified algorithm for the (t,t') method discussed below. The direction of polarization is taken to be perpendicular to the dipole for bent geometry and along the O-H axis of linear geometry and the geometry is kept fixed during the dynamics. The light used has a wavelength of 431 *nm* and an intensity of $2.2464 \times 10^{14} \text{ W/cm}^2$ with a 120 *a.u.* duration. The frequency used is close to the least absorbing frequency for water molecule and non-resonant to any of the transition for water molecule from ground to excited state. The physical properties like energy and population have then been computed as well during the dynamics.

3.1 (t,t') method for time dependent Schrödinger equation

The time dependent dynamics can be done using various methods available to solve the time dependent schrödinger equation: $\hat{H}\Psi = i\hbar\frac{\partial\Psi}{\partial t}$ One such method is the (t,t')[1] formalism where a new coordinate-t' is introduced in an extended Hilbert space such that the TDSE becomes,

$$i\hbar\left[\frac{\partial}{\partial t} + \frac{\partial}{\partial t'}\right]\Psi(r, t, t') = \hat{H}(r, t')\Psi(r, t, t') \quad (3.1)$$

Or we can write above equation as:

$$i\hbar\frac{\partial}{\partial t}\Psi(r, t, t') = \left[\hat{H}(r, t') - \frac{\partial}{\partial t'}\right]\Psi(r, t, t') \quad (3.2)$$

On the contour t=t', this equation can be written in the form of the general TDSE given as:

$$\hat{H}_F(r, t')\Psi(r, t, t') = i\hbar\frac{\partial\Psi(r, t, t')}{\partial t} \quad (3.3)$$

where, $\hat{H}_F(r, t') = \hat{H}(r, t') - \frac{\partial}{\partial t'}$ is the floquet Hamiltonian in t' coordinate. By floquet theorem, for time periodic Hamiltonians, the time periodic Fourier basis functions along with the spatial functions can be taken as a basis. The Hamiltonian for system in oscillating field is time periodic, therefore we can write initial wave function as:

$$\Psi(\vec{r}, t) = \sum_{k=-\infty}^{\infty} c_k(t)\psi_k(\vec{r}, t); \quad \psi_k(\vec{r}, t) = e^{-\frac{i}{\hbar}E_k^{QE}t}\phi_k(\vec{r}, t) \quad (3.4)$$

Here, E_k^{QE} are Quasienergies and ϕ_k are time periodic wavefunctions.

On substituting this in Eq. [3.3] we get:

$$\hat{H}_F(r, t')\phi_k(r, t) = \left[\hat{H}(r, t') - \frac{\partial}{\partial t'}\right]\phi_k(r, t) = E_k^{QE}\phi_k(r, t) \quad (3.5)$$

As can be seen from Eq. [3.5] that quasi-energies are the modified energy eigenvalue of floquet Hamiltonian for the modified system in oscillating fields.

Now we expand the floquet Hamiltonian eigenfunctions into a new basis of orthonormal time periodic functions with spatial part being the set of functions of field free Hamiltonian and temporal part by set of exponential function given by $e^{in\omega t}$ where n is the floquet channel index.

Therefore, we can write:

$$\phi_k(r, t) = \sum_{n=-\infty}^{\infty} \sum_{\alpha} \chi_{\alpha}(\vec{r}) e^{in\omega t}; \quad \hat{H}_o \chi_{\alpha}(\vec{r}) = E_{\alpha} \chi_{\alpha}(\vec{r}) \quad (3.6)$$

Where, \hat{H}_o is the field free Hamiltonian and $\chi_{\alpha}(\vec{r}), E_{\alpha}$ are the eigenfunction and eigenvalues respectively of field free Hamiltonian.

The full wavefunction can now be written as:

$$\Psi(\vec{r}, t) = \sum_{k=-\infty}^{\infty} \sum_{n=-\infty}^{\infty} \sum_{\alpha} c_k(t) e^{-\frac{i}{\hbar} E_k^{QE} t} \chi_{\alpha}(\vec{r}) e^{in\omega t} \quad (3.7)$$

The time evolution is of the form:

$$\Psi(r, t, t') = e^{-(i/\hbar) \hat{H}_F(r, t')(t-t_o)} \Psi(r, t_o, t')$$

From the solution physical properties can be calculated putting $t=t'$.

3.2 Electronic dynamics

The electronic dynamics of the linear and the bent geometry have been computed as shown in Fig.(3.1) in presence of a sine^2 envelope with 120 optical cycles, 120 *a.u.* duration with a Continuous Wave(CW) region of 40 *a.u.* duration in between the rise and fall of the laser with wavelength of 431 *nm* and an intensity of $2.2464 \times 10^{14} \text{ W/cm}^2$. The time dependent energy of the geometries have been calculated averaged in the CW region of the pulse. The results obtained show that the time averaged energy of the linear geometry is lower than that of the bent geometry by 0.04572 *Hartree* or 1.24 *eV*. This supports the fact that the linear geometry has been stabilized in the CW region of the pulse over the bent geometry. The time dependent calculation is done with fixed nuclear coordinate and therefore time averaged energy for the complete CW region of the pulse is required to characterize the stabilization. The max field strength is 0.08 *a.u.*.

The energy of the bent and linear geometry has remained below their respective ionization energy supporting the fact that no ionization will take place during the dynamics. The new states that are formed for the molecule in presence of the field are linear combinations of the excited states of field free molecule. During the propagation all the states are lifted in energy compared to the initial states for the field free molecule. The frequency used is non-resonant to any of the transition from ground electronic state to an excited electronic state of the molecule and the frequency is close to the minimum in absorption spectrum for water molecule thus achieving stabilization at high intensity regime.

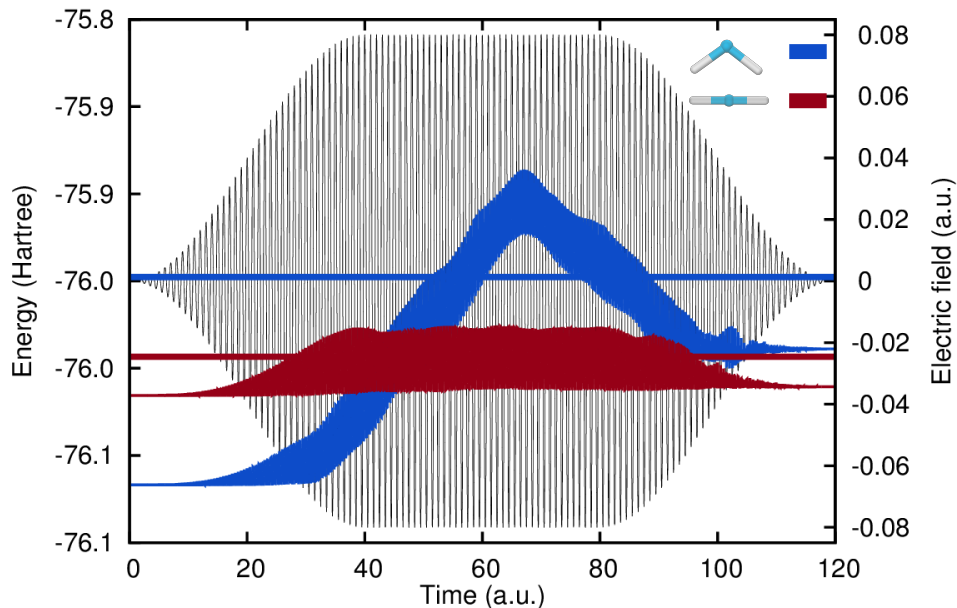


FIGURE 3.1: Time dependent electronic dynamics using modified algorithm of (t, t') method of bent geometry (blue plot) and linear geometry (red plot) in sine² envelope pulse with CW region with laser polarization perpendicular to dipole of bent geometry and along the O-H axis for linear geometry. The field (black plot) used has wavelength of 431 nm and a peak intensity of $2.2464 \times 10^{14} \text{ W/cm}^2$. The time averaged energy has also been marked for CW region of pulse. The linear geometry has been stabilized over bent geometry in CW region. The energy of the bent and linear geometry has remained below their respective ionization energy supporting the fact that no ionization will take place during the dynamics.

The dynamics of the intermediate geometries from bent to linear have also been computed as shown in Fig.(3.2) with the laser direction perpendicular to dipole of the geometries and laser with wavelength of 431 nm and an intensity of $2.2464 \times 10^{14} \text{ W/cm}^2$. The energy of some of the intermediate geometries have been shown below. The H-O-H angle has been marked in the dynamics. The energies of some intermediate geometries gets higher than their respective ionization potential like as shown for geometries with H-O-H angle 172.8° , 149.7° , 142.1° and 126.9° . For the other geometries the energy in dynamics is oscillatory and energy doesn't rise much in number. This again shows stability for some geometries in laser while instability of others.

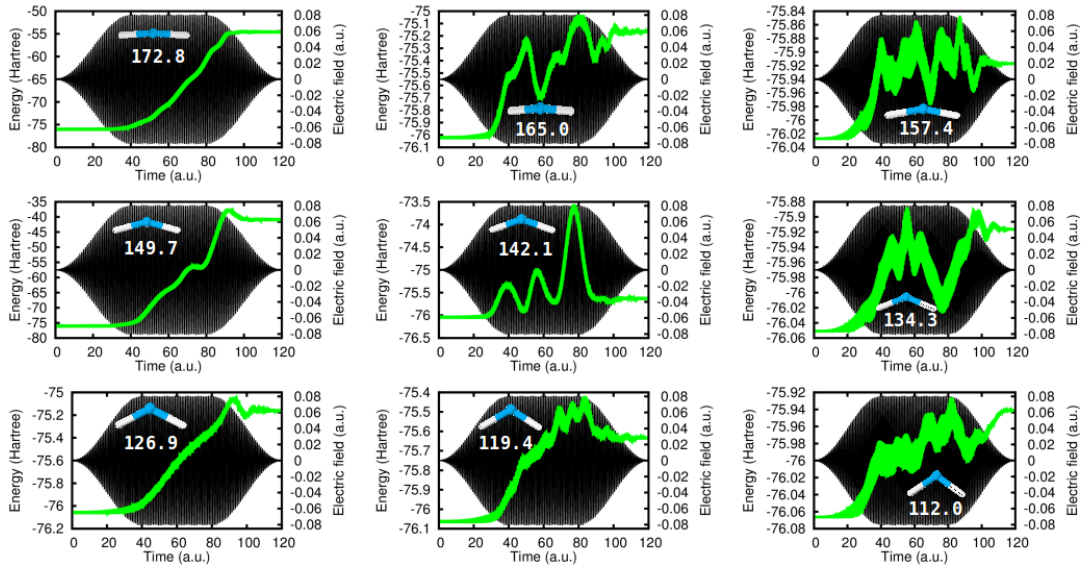


FIGURE 3.2: Time dependent electronic dynamics of some intermediate geometries (green plot) from bent to linear in sine^2 envelope pulse with CW region. The field (black plot) used has wavelength of 431 nm and an intensity of $2.2464 \times 10^{14} \text{ W/cm}^2$. The energy of geometry with H-O-H angle 172.8° , 149.7° , 142.1° and 126.9° goes very high than their respective ionization potential depicting their instability in laser.

The population of the ground and excited states has also been plotted for bent shown in Fig.(3.3a) and linear shown in Fig.(3.3b) geometry for the dynamics along with the laser field. The initial population resides in the ground state for both bent and linear geometry but as the field strength increases the excited states starts to populate. Since the frequency is chosen to be non-resonant to any of the excitation, the chances of population inversion decreases. But as the laser is intense the shifting of states in energy takes place. This shifting can lead to altering of energy levels and excitation energies leading to increase in population of excited states which takes place in the bent and linear geometry during the dynamics, but is more prominent in the bent geometry as can be seen in the plot. This is because the bent geometry energy level during the dynamics become resonant to laser wavelength and therefore some population of ground state excites to those levels. But, still the ground state is mostly populated in both the bent and the linear geometry. This suggests that no excitation or ionization is taking place during the dynamics.

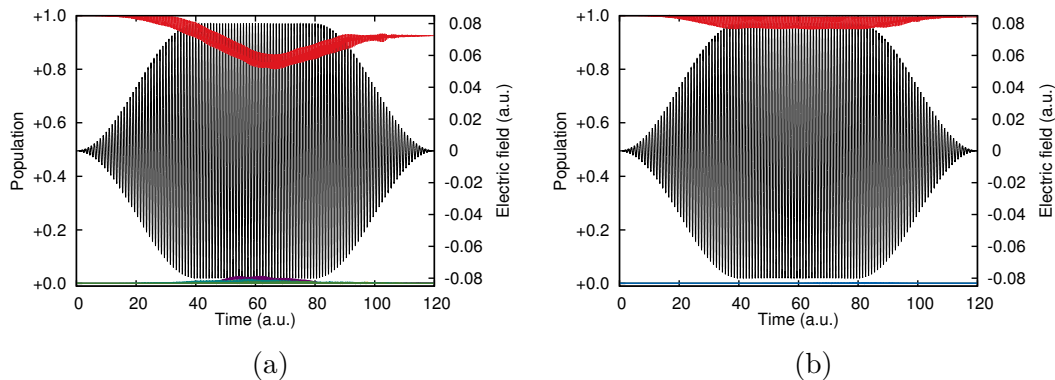


FIGURE 3.3: (a) Population of the ground and excited states for bent geometry. The red plot is the population for ground state and is highly populated during the dynamics. The black curve is the electric field with field strengths marked. The red plot is the population for ground state while the other plots are the excited states population. The population of some excited states increase during the dynamics after around $20 a.u.$ while ground state population declines. (b) Population of the ground and excited states for linear geometry. The red plot is the population for ground state while the other plots are the excited states population.

3.3 Conclusion

The time dependent electronic dynamics support the fact that the linear geometry has been stabilized over the bent geometry in the CW region of the laser. The direction of polarization is taken to be perpendicular to the dipole for bent geometry and along the O-H axis of linear geometry. The field has 120 optical cycles, $120 a.u.$ duration with $431 nm$ wavelength and an intensity of $2.2464 \times 10^{14} W/cm^2$. The energy in the dynamics has remained below ionization threshold. The ground state has also remained populated. This implies that a very small fraction of molecule is being ionized. The results from these calculations not only support the fact that lasers can be used to modify the structure or geometry of molecules but also that the transition states can be stabilized on top of the barrier in presence of intense oscillating fields.

References

- [1] U. Peskin and N. Moiseyev, *J. Chem. Phys.* **99**, 4590 (1993).
- [2] H. Sambe, *Phys. Rev. A* **7**, 2203 (1973).
- [3] J. S. Howland, *Mathematische Annalen* **207**, 315-335 (1974).

Appendix A

Numerical Method to solve Time dependent Schrödinger equation

A.1 Split operator method

For atom in electromagnetic radiation linearly polarized in z direction, the electronic Schrodinger equation in atomic units would be written as:

$$\left[\hat{T} + \hat{V}_{Ne} + \hat{V}_{ee} + \sum_{i=1}^n \hat{e}_z \cdot \vec{r}_i \epsilon_o \cos(\omega t) \right] \Psi_e(\vec{r}, t) = i \frac{\partial \Psi_e(\vec{r}, t)}{\partial t} \quad (\text{A.1})$$

The wavefunction can be expanded in the basis of time independent field free eigenfunctions. Thus,

$$\Psi_e(\vec{r}, t) = \sum_j C_j(t) \cdot \phi_j(\vec{r}) \quad (\text{A.2})$$

The time dependent coefficients of the field free states propagate as,

$$C_j(t + \Delta t) = e^{-i\hat{H}(\vec{r}, t) \cdot \Delta t} C_j(t) \quad (\text{A.3})$$

Now the time dependent part of the hamiltonian can be taken as perturbation. It is viable to write:

$$\hat{H}(\vec{r}, t) = \hat{H}_o(\vec{r}) + \hat{H}'(\vec{r}, t)$$

By Trotter theorem we can write the time evolution operator as,

$$e^{-i[\hat{H}_o + \hat{H}']\Delta t} = \lim_{M \rightarrow \infty} \left[e^{-i\hat{H}_o\Delta t/M} e^{-i\hat{H}'\Delta t/M} \right]^M \quad (\text{A.4})$$

Using a higher order split we can get better approximation to the time evolution operator. Here we have used a 7 order split. Using this we write.

$$e^{-i\hat{H}(\vec{r}, t)\Delta t} \approx e^{-ia_1\hat{H}_e(\vec{r})\Delta t} e^{-ib_1\hat{H}'(\vec{r}, t)\Delta t} e^{-ia_2\hat{H}_e(\vec{r})\Delta t} e^{-ib_2\hat{H}'(\vec{r}, t)\Delta t} \\ \times e^{-ia_2\hat{H}_e(\vec{r})\Delta t} e^{-ib_1\hat{H}'(\vec{r}, t)\Delta t} e^{-ia_1\hat{H}_e(\vec{r})\Delta t}$$